confirming that their resources cannot be recycled.

Supplemental Information

Supplemental Information including experimental procedures, a figure and a table can be found with this article online at http://dx.doi.org/10.1016/j.cub.2012.064.038.

Acknowledgments

We thank The Smithsonian Tropical Research Institute for providing facilities in Gamboa that allowed us to collect ant colonies and conduct the behavioural assays, Luke Holman and two anonymous reviewers for helpful comments on an earlier version of the manuscript, and the members of the Centre for Social Evolution for creating a pleasant working environment. This study was supported by The Danish National Research Foundation (J.J.B.), the German Academic Exchange Service DAAD (V.N.) and a Freia grant from the Faculty of Science, University of Copenhagen (P.d.E.).

References

1. Strassmann, J.E., and Queller, D.C. (2007). Insect societies as divided organisms: The complexities of purpose and cross-purpose. Proc. Natl. Acad. Sci. USA *104*, 8619–8626.
2. Boomsma, J.J. (2009). Lifetime monogamy and the evolution of eusociality. Phil. Trans. Biol. Sci. *364*, 3191–3207.
3. Cornwallis, C.K., West, S.A., Davis, K.E., and Griffin, A.S. (2010). Promiscuity and the evolutionary transition to complex societies. Nature *466*, 969–972.
4. Leadbeater, E., Carruthers, J.M., Green, J.P., Rosser, N.S., and Field, J. (2011). Nest inheritance is the missing source of direct fitness in a primitively eusocial insect. Science *333*, 874–876.
5. Hart, A.G., and Ratnieks, F.L.W. (2005). Crossing the taxonomic divide: conflict and its resolution in societies of reproductively totipotent individuals. J. Evol. Biol. *18*, 383–395.
6. Gordon, D.M. (1996). The organization of work in social insect colonies. Nature *380*, 121–124.
7. Nielsen, M.G. (1978). Production of sexuals in nests of *Lasius flavus* (Forst.) (Hymenoptera: Formicidae). Nat. Jutl. *20*, 251–254.
8. Dijkstra, M.B., and Boomsma, J.J. (2007). The economy of worker reproduction in *Acromyrmex* leafcutter ants. Anim. Behav. *74*, 519–529.
9. Keller, L. (1991). Queen number, mode of colony founding, and queen reproductive success in ants (Hymenoptera, Formicidae). Ethol. Ecol. Evol. *3*, 307–316.
10. De Fine Licht, H.H., and Boomsma, J.J. (2010). Forage collection, substrate preparation and diet composition in fungus-growing ants. Ecol. Entomol. *35*, 259–269.

[1]Centre for Social Evolution, Department of Biology, University of Copenhagen, 2100 Copenhagen, Denmark. [2]Biology I, University of Freiburg, Hauptstraße 1, 79104 Freiburg, Germany. [3]Laboratoire d'Ethologie Expérimentale et Comparée (LEEC), Université Paris 13, 93430 Villetaneuse, France.
*E-mail: volker.nehring@biologie.uni-freiburg.de

The first World Cell Race

Paolo Maiuri[1], Emmanuel Terriac[1], Perrine Paul-Gilloteaux[1], Timothée Vignaud[2], Krista McNally[3], James Onuffer[3], Kurt Thorn[3], Phuong A. Nguyen[4], Nefeli Georgoulia[4], Daniel Soong[5], Asier Jayo[5], Nina Beil[6], Jürgen Beneke[6], Joleen Chooi Hong Lim[7], Chloe Pei-Ying Sim[7], Yeh-Shiu Chu[7], WCR participants[8], Andrea Jiménez-Dalmaroni[9], Jean-François Joanny[9], Jean-Paul Thiery[7], Holger Erfle[6], Maddy Parsons[5], Timothy J. Mitchison[4], Wendell A. Lim[3], Ana-Maria Lennon-Duménil[10], Matthieu Piel[1,*], and Manuel Théry[2,*]

Motility is a common property of animal cells. Cell motility is required for embryogenesis [1], tissue morphogenesis [2] and the immune response [3] but is also involved in disease processes, such as metastasis of cancer cells [4]. Analysis of cell migration in native tissue *in vivo* has yet to be fully explored, but motility can be relatively easily studied *in vitro* in isolated cells. Recent evidence suggests that cells plated *in vitro* on thin lines of adhesive proteins printed onto culture dishes can recapitulate many features of *in vivo* migration on collagen fibers [5,6]. However, even with controlled *in vitro* measurements, the characteristics of motility are diverse and are dependent on the cell type, origin and external cues. One objective of the first World Cell Race was to perform a large-scale comparison of motility across many different adherent cell types under standardized conditions. To achieve a diverse selection, we enlisted the help of many international laboratories, who submitted cells for analysis. The large-scale analysis, made feasible by this competition-oriented collaboration, demonstrated that higher cell speed correlates with the persistence of movement in the same direction irrespective of cell origin.

The race track consisted of 4 μm- and 12 μm-wide fibronectin lines printed in multi-well glass-bottomed cell-culture wells (see Supplemental Experimental Procedures and Figure S1A in the Supplemental Information available online); 54 different cell types from various animals and tissues were provided by 47 laboratories. Genotypically, cells were wild type, transformed or genetically engineered (Table S1). The cells were distributed to six organizing laboratories (two in the USA, and one each in the UK, France, Germany and Singapore), who prepared cell-culture stocks using the frozen samples received from participating laboratories and plated these onto the race tracks under identical culture conditions. Cells were allowed to adhere overnight and cell motility was recorded for 24 hours using an inverted video microscope (Figure 1B, Movie S1). Cell morphology (length, shape, symmetry, and nucleus position) varied greatly from one cell type to another (Figure 1A). Cell nuclei were stained by incubating live cells with 5 ng/ml Hoechst dye diluted in normal growth medium. Cell displacements were monitored every 10 minutes. Nuclei images were segmented and geometric centers were tracked with a global minimization algorithm in order to track automatically individual cell displacements (see Supplemental Experimental Procedures and Figure S1B). The motility of over 7,000 cells was compared, with an average of 130 cells analyzed per cell type. Detailed statistical analyses were used to characterize cell motility parameters for each cell type (see http://www.worldcellrace.com/ResultFiles).

The mean instantaneous speed of individual cells is computed by averaging the cell displacements between consecutive frames over time. The distribution of mean instantaneous speeds for each cell type was asymmetric (Figure 1C) and non-Gaussian (Figure S1C). Interestingly, we observed that a higher mean speed for a given cell type did not reflect a global shift of the speed distribution, but rather the spreading of the distribution due to the presence of faster moving cells (Figure 1C and Figure S1C). In order to identify the 2011 World Cell Race winner, only cells with an effective overall displacement of at least

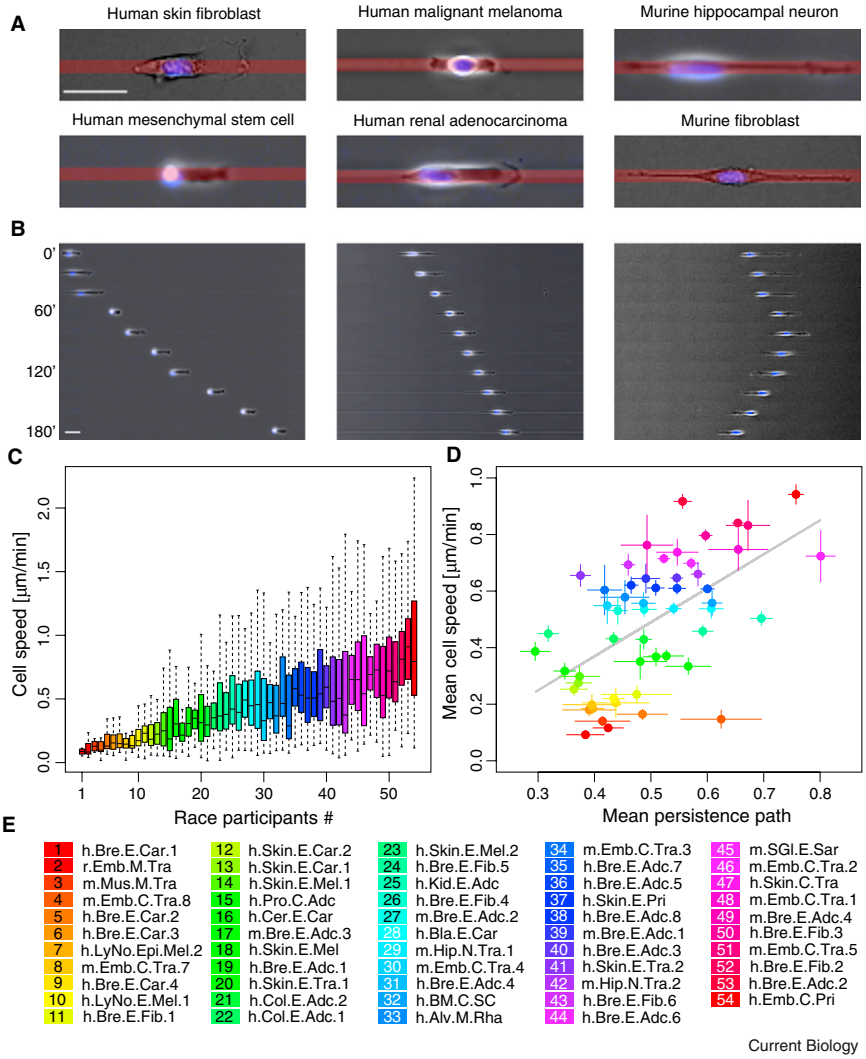

Figure 1. Cell speed and motion persistence on race tracks.
(A) Images illustrating cell shape variability on micropatterned tracks. (B) Kymographs illustrating different types of cell motility. Scales bars represent 50 µm. (C) Cell speed distributions represented with quartile diagrams for all participants. (D) Mean cell speeds plotted versus mean persistence . Bars correspond to standard deviation. Pearson correlation coefficient of the linear fit is 0.58. All cells analyzed are listed and color coded. (E) Color-coded participating cell types list: cell type – organism.source.tissue.tumor. Organisms: human (h), mouse (m), rat (r). Sources: embryo (Emb), alveola (Alv), bladder (Blad), bone marrow (BM), breast (Bre), cervix (Cer), colon (Col), hippocampus (Hip), kidney (Kid), lymph node (LyNo), muscle (Mus), prostate (Pro), salivary glands (SGl), skin. Tissues: epithelial (E), connective (C), muscle (M), nervous (N). Tumors: transformed (Tra), adenocarcinoma (Adc), carcinoma (Car), fibroma (Fib), melanoma (Mel), primary (Pri), rhabdomyosarcoma (Rha), sarcoma (Sar), stem cells (SC).

350 µm were considered. This cut-off was only reached by 26 of the 54 cell types. The highest migration speed was recorded at 5.2 µm/min by a human embryonic mesenchymal stem cell (Movie S2).

Cell displacements on lines can be described by a 1D correlated random walk [7], simply derived from the 2D model, in which cells are more likely to move in the direction of the immediately preceding movement conserving their polarity. This can be quantified by a *persistence probability* (p) for a cell to maintain its direction of motion and keep the same *front* and *rear*. For each cell type, we measured the number of cell steps between two motion reversals, i.e. the number of consecutive time intervals during which cells kept moving in the same direction (Figure S1E). To calculate p, histograms built from the number of cell steps were fitted to the 1D correlated random walk theory (Figure S1D). A persistence path, defined as the ratio of the effective maximum displacement to the actual trajectory length, was further calculated to obtain a macroscopic measure of p (Figure S1F). This ratio was strongly correlated with the persistence probability (Figure S1G). Persistence path distributions for the 54 cell types were typically non-Gaussian (Figure S1H). Strikingly, the overall mean speeds for all cell types correlated well with their mean persistence path (Figure 1D), implying that fast-moving cell types (mean cell speed >0.7 µm/min) displayed high mean persistence path (>0.5). Cells moving rapidly, but only backwards and forwards, were not observed.

Given the large and diverse sample of cell types, this result may reveal a conserved mechanism that allows the coupling of the machinery controlling cell polarity (responsible for persistent oriented motion) to the one regulating instantaneous cell speed. Future experiments aimed at unraveling the associated molecular mechanisms shall now be performed.

Together, the results generated by the first World Cell Race highlight how scientific games involving large-scale experiments can lead to the identification of novel and relevant biological processes, which may otherwise escape observation.

Supplemental Information

Supplemental Information includes experimental procedures, one figure, one table and two movies and can be found with this article online at http://dx.doi.org/10.1016/j.cub.2012.07.052.

Acknowledgments

We thank all the participants who sent cells to the inaugural World Cell Race (listed in Table S1). We thank the Société de Biologie Cellulaire de France for its financial support and the American Society for Cell Biology for the organization of the session dedicated to the race during the 2011 annual meeting. We thank our industrial partners, Cytoo and Nikon Instruments, who provided the micropatterned substrates and the imaging platforms, respectively.

P. Maiuri received a fellowship from the Fondation pour la Recherche Médicale, M. Parsons is funded by a Royal Society University Research Fellowship, H. Erfle and J. Beneke by the CellNetworks-Cluster of Excellence (EXC81), J. Onuffer, W.A. Lim and T.J. Mitchison by the NIH (PN2EY016546, GM23928), A. Lennon-Duménil and M. Piel by the ANR and Innabiosanté (09-PIRI-0027-PCVI and

MICEMICO), M. Théry by the INCA (PLBIO-2011-141).

References

1. Keller, P.J., Schmidt, A.D., Wittbrodt, J., and Stelzer, E.H.K. (2008). Reconstruction of zebrafish early embryonic development by scanned light sheet microscopy. Science *322*, 1065–1069.
2. Rembold, M., Loosli, F., Adams, R.J., and Wittbrodt, J. (2006). Individual cell migration serves as the driving force for optic vesicle evagination. Science *313*, 1130–1134.
3. Faure-André, G., Vargas, P., Yuseff, M.-I., Heuzé, M., Diaz, J., Lankar, D., Steri, V., Manry, J., Hugues, S., and Vascotto, F., *et al.* (2008). Regulation of dendritic cell migration by CD74, the MHC class II-associated invariant chain. Science *322*, 1705–1710.
4. Gligorijevic, B., Wyckoff, J., Yamaguchi, H., Wang, Y., Roussos, E.T., and Condeelis, J. (2012). N-WASP-mediated invadopodium formation is involved in intravasation and lung metastasis of mammary tumors. J. Cell Sci. *125*, 724–734.
5. Pouthas, F., Girard, P., Lecaudey, V., Ly, T.B.N., Gilmour, D., Boulin, C., Pepperkok, R., and Reynaud, E.G. (2008). In migrating cells, the Golgi complex and the position of the centrosome depend on geometrical constraints of the substratum. J. Cell Sci. *121*, 2406–2414.
6. Doyle, A.D., Wang, F.W., Matsumoto, K., and Yamada, K.M. (2009). One-dimensional topography underlies three-dimensional fibrillar cell migration. J. Cell Biol. *184*, 481–490.
7. Codling, E.A, Plank, M.J., and Benhamou, S. (2008). Random walk models in biology. J. R. Soc. Interface *5*, 813–834.

[1]Institut Curie, CNRS, UMR144, 75248, Paris, France. [2]Institut de Recherches en Sciences et Technologies pour le Vivant, CEA, UJF, CNRS, INRA, 38054, Grenoble, France. [3]Department of Cellular and Molecular Pharmacology, UCSF, San Francisco, CA 94158, USA. [4]Harvard Medical School, Systems Biology, Boston, MA 02115, USA. [5]Kings College London, SE1 1UL London, UK. [6]BioQuant, Heidelberg University, Germany. [7]Institute of Molecular and Cell Biology, A*Star, Proteos, 138673, Singapore. [8]World Wide, listed in Supplemental Information. [9]Institut Curie, CNRS, UMR168, 75248, Paris, France. [10]Institut Curie, INSERM, U639, 75248, Paris, France.
*E-mail: matthieu.piel@curie.fr, manuel.thery@cea.fr

Global distribution of a wild alga revealed by targeted metagenomics

Alexandra Z. Worden[1,*], Jan Janouskovec[2], Darcy McRose[1], Augustin Engman[1], Rory M. Welsh[1], Stephanie Malfatti[3], Susannah G. Tringe[3], and Patrick J. Keeling[2]

Eukaryotic phytoplankton play key roles in atmospheric CO_2 uptake and sequestration in marine environments [1,2]. Community shifts attributed to climate change have already been reported in the Arctic ocean, where tiny, photosynthetic picoeukaryotes (≤3 μm diameter) have increased, while larger taxa have decreased [3]. Unfortunately, for vast regions of the world's oceans, little is known about distributions of different genera and levels of genetic variation between ocean basins. This lack of baseline information makes it impossible to assess the impacts of environmental change on phytoplankton diversity, and global carbon cycling. A major knowledge impediment is that these organisms are highly diverse, and most remain uncultured [2]. Metagenomics avoids the culturing step and provides insights into genes present in the environment without some of the biases associated with conventional molecular survey methods. However, connecting metagenomic sequences to the organisms containing them is challenging. For many unicellular eukaryotes the reference genomes needed to make this connection are not available. We circumvented this problem using at-sea fluorescence activated cell sorting (FACS) to separate abundant natural populations of photosynthetic eukaryotes and sequence their DNA, generating reference genome information while eliminating the need for culturing [2]. Here, we present the complete chloroplast genome from an Atlantic picoeukaryote population and discoveries it enabled on the evolution, distribution, and potential carbon sequestration role of a tiny, wild alga.

We assembled a complete chloroplast genome from a coherent picoeukaryote population sorted from the Gulf Stream Current. The sorting step reduced bioinformatic complexity to a level where high quality *de novo* sequence assembly was possible. The resulting circular plastid genome was 91,306 bp, 35% G+C and encoded 106 proteins, 27 tRNAs, an rRNA operon as well as other features (Figure S1 in Supplemental Information, published with this article online). Multiple lines of evidence demonstrate this genome is from a member of the Pelagophyceae, a recently discovered phytoplankton class [4]. Complete plastid genomes are available from two cultured Pelagophyceae, the brown-tide forming *Aureococcus anophagefferens* and *Aureoumbra lagunensis*. Genome organization in the uncultured pelagophyte was similar to *Aureococcus*, and more divergent from *Aureoumbra* (Figure 1A), consistent with evolutionary relationships deduced from our 105 plastid-protein phylogeny (Figure S2). The uncultured pelagophyte encoded all *Aureococcus* genes plus one (*ycf45*) of *Aureoumbra*'s five additional proteins. All three Pelagophyceae encoded a 267 residue protein with multiple predicted transmembrane domains not seen in any other organisms based on tblastn and blastp against the full GenBank repository. Comparisons with the best-sampled protein-encoding pelagophyte plastid gene, *rbcL*, showed the uncultured population was most similar to *Pelagomonas calceolata* (99.0% nucleotide identity, ≤95.2% to other Pelagophyceae). The 16S rRNA gene, which is highly conserved across genera, had 100% identity to partial sequences available for *P. calceolata*. The uncultured population may therefore be *P. calceolata*, but based on extant sampling we call it 'wild *Pelagomonas*'.

With the plastid genome in hand, we addressed the distribution and ecological significance of this lineage. The complete set of coding regions from the chloroplast genome was compared with marine metagenomic samples using a cutoff of 97.0% nucleotide identity. We found that the wild *Pelagomonas*